1989

Atmospheric Emission Models: Confrontation between Observational Data and Predictions in the 2.5 to 300 GHz Frequency Range

Luigi Danese

Bruce Partridge
Haverford College, bpartrid@haverford.edu

1989

Atmospheric Emission Models: Confrontation between Observational Data and Predictions in the 2.5 to 300 GHz Frequency Range

L. Danese

R. Bruce Partridge
Haverford College

THE ASTROPHYSICAL JOURNAL, 342:604–615, 1989 July 1

ATMOSPHERIC EMISSION MODELS: CONFRONTATION BETWEEN OBSERVATIONAL DATA AND PREDICTIONS IN THE 2.5–300 GHz FREQUENCY RANGE

L. DANESE
Dipartimento di Astronomia, Padova, Italy
AND
R. B. PARTRIDGE
Haverford College, Haverford, Pennsylvania
Received 1988 May 31; accepted 1988 November 4

ABSTRACT

Data on atmospheric zenith opacity obtained from a high-altitude (3.8 km) site are compared with detailed atmospheric models available in the literature. The comparison is successful and useful; in fact, we are able to discriminate among various proposed solutions for both the O_2 and the H_2O continuum. Moreover, the data at high frequencies indicate that the models probably underestimate by 20% the strength of the H_2O line at 22 GHz. Also, the 60 GHz O_2 band contribution to the total opacity must be reevaluated by 15%. The oxygen and water vapor opacities in the 3 cm–0.8 mm range are computed with the best-fitting model for Mauna Kea, Kitt Peak, and the South Pole.

Subject headings: Earth: atmosphere — opacities — radio sources: general

I. INTRODUCTION

The absorption and consequent reemission of microwave radiation by the Earth's atmosphere is a well-known phenomenon. The effects on radio-wave propagation have been analyzed in detail, particularly in connection with space communications. Nevertheless, we have been led to reassess the problem because of the critical role played by the emission from the atmosphere in programs designed to measure the temperature of the cosmic background radiation when those programs are carried out beneath some or most of the atmosphere (for recent reports see Weiss 1980; Peterson, Richards, and Timusk 1985; Smoot *et al.* 1985, 1987; Johnson and Wilkinson 1987). We note also that both ground-based searches for anisotropies in the microwave background and millimeter-wave observations are strongly affected by variable emission from the atmosphere.

As part of a program to measure the spectrum of the cosmic background radiation at five wavelengths (Smoot *et al.* 1983, 1985), a series of measurements of the contributions of the Earth's atmosphere was carried out at White Mountain, California, at 3800 m altitude. In 1982 June and July atmospheric emission measurements were made at 2.5 GHz (Sironi, Inzani, and Ferrari 1984), at 9.4 GHz (Partridge *et al.* 1984), at 10 GHz (Friedman *et al.* 1984), and at 33 and 90 GHz (De Amici *et al.* 1984). In 1983 August and September observations were performed at 4.75 GHz (Mandolesi *et al.* 1986) and repeated at 9.4 GHz (present paper), at 10 GHz (Friedman 1984) at 33 GHz (De Amici *et al.* 1985), and at 90 GHz (Witebsky *et al.* 1986). Moreover, in the summer months of 1984 simultaneous measurements of atmospheric emission at 10, 33, and 90 GHz were made on White Mountain as well as at a sea-level site (Costales 1984; Costales *et al.* 1986). The results were exploited to look for systematic errors in the evaluation of the atmospheric contribution to the antenna temperature when computing the cosmic background radiation temperature (see, e.g., Mandolesi *et al.* 1986). More recently (for a summary see Smoot *et al.* 1987), new measurements have been obtained at 3.7 GHz (De Amici *et al.* 1988), again at 10 GHz (Kogut *et al.* 1988), and at 90 GHz (Bersanelli and Witebsky 1989, reported in Smoot *et al.* 1987).

This large body of data also allows a new and well-substantiated discussion of the atmospheric emission, which is the aim of this paper: low-frequency measurements are good tests for dry air emission, whereas at high frequencies (33 and 90 GHz) the water vapor contribution can be tested. In § II of this paper we briefly describe the model for atmospheric attenuation that we chose as a reference, and we review the assumptions and steps involved in calculating the models. In § III we first discuss the low-frequency data collected at White Mountain in 1982 and 1983; for high-frequency data we will use both the 1983 and the 1984 observations. The comparison with the reference model is then presented, and we propose some adjustments to the reference model in § IV. In § IV the adjusted model is also compared with previous data collected from the literature, and the confrontation of the model with the data is extended also to the millimeter and submillimeter regions. Finally, in § V we make predictions of atmospheric attenuation in the 10–380 GHz frequency range for three interesting astronomical sites, Mauna Kea, Kitt Peak, and the Amundsen-Scott Station at the South Pole.

II. THE REFERENCE MODEL

Models for the propagation of millimeter and centimeter waves may be used to compute attenuation, delay, and noise properties of clear air for frequencies up to 1000 GHz and for observing sites with altitudes ranging from sea level to 30 km (Liebe 1981). The models require as input variables the distribution with the altitude of temperature, pressure, and water vapor density, and a parametric description of the absorption lines and continuum spectra of O_2 and H_2O.

If we adopt the hypothesis of a nonscattering and nonrefracting atmosphere in thermal equilibrium, we may write the equation of transfer for signal propagation from outside the atmosphere to an observer at altitude H_{obs} in terms of

antenna temperature as follows (following Waters 1976):

$$T(H_{obs}) = T_\infty \exp\,[-\tau_\nu(0, s_{obs})] + \int_0^{s_{obs}} T_{phys}(s') \exp\,[-\tau_\nu(s' - s_{obs})] k_\nu(s')\, ds' , \quad (1)$$

where T_∞ is the antenna temperature of the signal outside the atmosphere, and we use s to represent the distance traveled by the signal through the atmosphere to reach an altitude h. Thus $s = H_{atm} - h$, where H_{atm} is the altitude beyond which there is effectively no absorption. T_{phys} here is given by $T_{phys} = c^2 B_\nu(T)/2k_B \nu^2$, where $B_\nu(T)$ is the Planck function and we write k_B for Boltzmann's constant; in the Rayleigh-Jeans region this is identical with the physical temperature of the atmosphere at s'. Finally, $k_\nu(s)$ is the volume attenuation rate at s and frequency ν, and $\tau_\nu(s', s)$ is the optical depth between s' and s,

$$\tau_\nu(s', s) = \int_{s'}^{s} k_\nu(s'')ds'' . \quad (2)$$

Attenuation rates are usually expressed in cm^{-1} or dB km^{-1} ($1\ cm^{-1} = 4.34 \times 10^5$ dB km^{-1}). The optical depth or total attenuation, which is a nondimensional quantity, may be expressed in nepers or decibels (1 neper = 4.34 dB).

In the following we are interested in the atmospheric emission and particularly in the determination of the second term on the right-hand side of equation (1), i.e.,

$$T_{atm}(H_{obs}, \nu) = \int_0^{s_{obs}} T_{phys}(s') \exp\,[-\tau_\nu(0, s')] k_\nu(s') ds' = \bar{T}_{phys}(H_{obs}, \nu)\{1 - \exp\,[-\tau_\nu(0, s_{obs})]\} , \quad (3)$$

where $T_{atm}(H_{obs}, \nu)$ is the contribution of the atmosphere to the observed signal at frequency ν expressed in antenna temperature, and $\bar{T}_{phys}$ is an effective average physical temperature we can derive using the above relations after an exact integration of T_{atm}. To compute this quantity we need to know both the physical properties of the atmosphere (i.e., how temperature, pressure, and composition vary with the altitude) and the volume absorption coefficient, k_ν.

In our calculations we used the physical properties of the atmosphere as specified by the various model atmospheres given by McClatchey *et al.* (1972). We took into account only oxygen and water vapor, neglecting ozone and other minor constituents, because we are mainly interested in atmospheric absorption and emission in the window regions between spectral lines. Different physical models for the atmosphere have been tried, and we find that our results do not depend significantly on the specific model.

The general expression for the absorption coefficient k_ν contains a part depending on spectral lines $(k_\nu)_{lm}$ and a continuum part $(k_\nu)_c$ which must be added to the selected resonance lines in order to reproduce the atmospheric spectrum in window regions between the lines.

The absorption coefficient in a transition between states l and m may be written as

$$k_{lm} = 0.182 \nu S_{lm} F(\nu, \nu_{lm})\ \text{dB km}^{-1} , \quad (4)$$

where ν is the frequency in GHz, ν_{lm} is the frequency corresponding to the energy transition, S_{lm} is the line strength in kHz, and F is the line shape in GHz^{-1} (Liebe 1984).

The line-shape function is essentially determined by collisional interactions among molecules for altitudes up to 70 km (Waters 1976). Thermal and natural broadening are negligible in our case, because the relative contribution to the emission of atmospheric layers at altitudes greater than 40 km is much less than 10^{-3} of the values computed at 4 km.

Van Vleck and Weisskopf (1945) and Gross (1955) proposed different line shapes, both obtained by treating absorbers as classical harmonic oscillators. These line shapes have been used for a long time in atmospheric studies, both for their rather good agreement with the data and for their simple form.

Quantum-mechanical procedures in computing line shapes have also been exploited with different levels of approximation by many authors (see Lam 1977 for a brief review). In particular, Rosenkranz (1975), using the impact theory of overlapping lines, worked out a first-order approximation which in Liebe's (1985) notation is

$$F(\nu, \nu_{lm}) = \left(\frac{\nu}{\nu_{lm}}\right)\left[\frac{\gamma - (\nu - \nu_{lm})\delta}{(\nu - \nu_{lm})^2 + \gamma^2} + \frac{\gamma - (\nu_{lm} + \nu)\delta}{(\nu_{lm} + \nu)^2 + \gamma^2}\right] , \quad (5)$$

where ν_{lm} is the line-center frequency, γ is the width of the line, and δ is the overlap correction.

a) *Attenuation Coefficient of* H_2O

In the calculations of the attenuation coefficient k_ν for H_2O, we have to take into account the contributions of water vapor lines, of additional absorption far from the line centers, and finally of liquid water droplets, which may be present even for clear sky conditions:

$$(k_\nu)_w = \Sigma[(k_\nu)_{wv}]_{lm} + (k_\nu)_{wvc} + (k_\nu)_{lw} . \quad (6)$$

If we are interested in k_ν for frequencies lower than 500 GHz, we can get a very good description of the water vapor line contribution using only the 30 lines of lowest frequency. Strengths S and widths γ are parameterized as follows by Liebe (1985):

$$S = b_1 e\theta^{3.5} \exp\,[b_2(1 - \theta)]\ \text{kHz} , \quad (7)$$

$$\gamma = b_3(p\theta^{0.8} + 4.80e\theta)\ \text{GHz} , \quad (8)$$

where $\theta = 300/T(\text{K})$ is the relative inverse temperature parameter, p(kPa) is the dry air pressure, e(kPa) is the partial water vapor pressure, and b_1, b_2, and b_3 are parameters derived from the Air Force Geophysical Laboratory (AFGL) tape (Rothman *et al.* 1983). The list of the line frequencies and parameters is reported by Liebe (1985). For water vapor the interference coefficients vanish, since overlap corrections are not needed (Lam 1977).

The major contribution to the attenuation coefficient for frequencies below 300 GHz comes from the 22.235, 183.31, and 325.153 GHz lines. Other H_2O line data bases have been produced (Flaud, Camy-Peyret, and Toth 1981; Poynter and Pickett 1981; Mizushima 1982).

The summation of the water vapor line contributions gives values of k_ν which agree with the observed absorption only near the peaks of water vapor lines. In the windows between lines, that is, at wavelengths normally used for astronomical observations, the observed attenuations are 2–5 times larger than those predicted on the basis of the line contributions alone. This discrepancy is known as the problem of the excess water vapor absorption (EWA). An extensive discussion of the problem on both the experimental and the theoretical side can be found in the volume *Atmospheric Water Vapor* (Deepak, Wilkerson, and Ruhnke 1980). Several authors have proposed empirical corrections in the form of a water vapor continuum

to reconcile the computed absorptions with the measured values. The differences among the proposed corrections are often significant, and we shall see that this fact is due largely to the different line shapes adopted by the various authors. An excellent summary of the present state of the problem is given by Liebe (1984), who presents corrections proposed by Gaut and Rafenstein (1971), by Burch (1982), by Zrazhevskiy (1976), and by Zammit and Ade (1981). He also proposes a correction based on new laboratory data and on a refined calculation of the line contributions. In our reference model we use this last version of the continuum attenuation:

$$(k_\nu)_{\rm wvc} = (2.55 \times 10^{-7} ep\theta^{2.5} + 9.84 \times 10^{-6} e^2\theta^{5.5})\nu^2 \text{ dB km}^{-1} . \quad (9)$$

In §§ III and IV we will further discuss some aspects of the water vapor continuum problem on the basis of the data reported here.

We examined also the contribution to the attenuation coming from liquid water droplets with radii smaller than 20 μm (cloud or fog aerosols). The attenuation by droplets is obtained with the Rayleigh absorption approximation (Liebe 1981):

$$(k_\nu)_{\rm lw} = 0.82 w_{\rm lw} \epsilon''/[(\epsilon' + 2)^2 + \epsilon''^2] \text{ dB km}^{-1} , \quad (10)$$

where $w_{\rm lw}$ is the liquid water concentration in g m^{-3} and ϵ' and ϵ'' are the dielectric constants for water (Chang and Wilheit 1979).

Apart from the lines, the absorption due to H_2O is strongly increasing with frequency (see eq. [9]), and this is the reason why millimeter observations are usually made from dry and high-altitude sites with the lowest possible water vapor concentration.

b) *Oxygen Attenuation Coefficient*

Unlike the H_2O molecule, the oxygen molecule has no electric dipole moment. Hence, spectral lines at microwave frequencies are generated by magnetic dipole moments arising from the combined spins of two unpaired electrons in the $^3\Sigma^-$ ground state of the molecule; particularly interesting for us are the band of spin-rotation spectral lines near 60 GHz (0.5 cm wavelength) and a single line at 118 GHz ($\lambda = 0.25$ cm), but transitions between different rotational states of O_2 also produce spectral lines at wavelengths $\lambda \ll 0.08$ cm.

In the atmosphere the O_2 molecule is abundant (2.095×10^5 ppm in volume) and well mixed with the other gases; its large abundance ensures the importance of oxygen attenuation even though magnetic transitions are typically 10^4 times less intense than electric dipole transitions.

Van Vleck (1947) first described the basic characteristics of the spectrum of O_2 in its ground state. More recently good agreement with atmospheric attenuation measurements at various altitudes below 12 km was obtained by Reber (1972) in the 42–72 GHz frequency range by summing the individual transitions. In 1975 Rosenkranz, using a first-order approximation to the impact theory of overlapping spectral lines, managed to fit Reber's data at all altitudes within an average rms error of 6%. Liebe *et al.* (1977) gave an experimental confirmation of Rosenkranz's theory and determined the strengths, width parameters, and interference coefficients of 21 lines in the O_2 spectrum. The dependences on pressure and temperature of the strengths S, widths γ, and interference coefficients δ (called also "overlap corrections") are parameterized in the following way:

$$S = a_1 p\theta^3 \exp [a_2(1 - \theta)] \text{ kHz} , \quad (11)$$

$$\gamma = a_3(p\theta^{0.8 - a_4} + 1.1e\theta) \text{ GHz} , \quad (12)$$

$$\delta = a_5 p\theta^{a_6} . \quad (13)$$

Liebe (1985) lists the parameters $a_1, \ldots, a_6$ for 48 lines with frequencies ranging from 49.4524 to 834.145 GHz; we make use of this list for our reference model. Here, as in equations (7) and (8), e is the partial water vapor pressure.

As for water vapor, a continuum absorption monotonically increasing with frequency must be added to the O_2 resonance line absorption. This nonresonant absorption is connected with the nonvanishing probability for $\Delta J = 0$ transitions (J is the total angular momentum quantum number). Expressions for this term have been proposed by Van Vleck (1947), Rosenkranz (1975), and Smith (1981). A generalized version of Van Vleck's expression has recently been proposed (Liebe 1985):[1]

$$(k_\nu)_{\rm oxc} = \left(1.12 \times 10^{-4} p\theta^2 \frac{\tau_0}{\tau_0^2 + \nu^2} + 3.49 \times 10^{-11} p^2\theta^{2.5}\right)\nu^2 \text{ dB km}^{-1} . \quad (14)$$

The width parameter τ_0 for the O_2 continuum can be represented in the same way as for the line width:

$$\tau_0 = a(p + 1.1e)\theta^b . \quad (15)$$

As we shall see, our low-frequency measurements are able to add important constraints on the value of τ_0. In our reference model we choose $a = 0.0056$ and $b = 1.05$ (see following section).

Unlike the case for water vapor, we expect that the oxygen contribution to the optical depth will depend essentially only on the altitude of the observing sites and much less on the weather conditions.

To summarize, the reference model we employ coincides with the "millimeter propagation model" of Liebe (1985) as far as the water vapor attenuation is concerned, but differs in the expression used for the O_2 continuum attenuation.

III. OBSERVATIONAL DATA BASE AND COMPARISON WITH THEORY

As noted in § I above, our measurements of $T_{\rm atm}$ were made as part of a program to remeasure the spectrum of the cosmic background radiation at five wavelengths (Smoot *et al.* 1985). Detailed descriptions of the apparatus employed by various groups in the White Mountain collaboration may be found in Sironi, Inzani, and Ferrari (1984) for the 2.5 GHz results, in Mandolesi *et al.* (1984, 1986) for the 4.75 GHz results, in partridge *et al.* (1984) for the 9.4 GHz measurements of $T_{\rm atm}$, in Friedman *et al.* (1984) for the 10 GHz results, and in De Amici *et al.* (1984, 1985) and Witebsky *et al.* (1986) for the 33 and 90 GHz results. All these experiments employed corrugated horn antennas with very low sidelobes; beamwidths were of order 10° (see papers cited above). Calibration was provided by a

[1] In his 1985 paper, Liebe adds a high-frequency damping term $[1 + (\nu/60)^2]^{-1}$ to the first term on the right-hand side of eq. (14), as suggested by Stankevich (1974). For reasons explored in § IV*b* below, we omit this high-frequency damping term in our reference model.

liquid helium cold load in overmoded waveguide (see Smoot *et al.* 1983). Further T_{atm} observations at White Mountain were made in 1984 at 10, 33, and 90 GHz (Costales 1984; Costales *et al.* 1986); and more recently at 3.7, 10, and 90 GHz (see De Amici *et al.* 1988, Kogut *et al.* 1988, and Smoot *et al.* 1987, respectively).

Measurements of the atmospheric contribution T_{atm} were made in the usual fashion by measuring antenna temperature as the beam was tipped from the zenith to a set of different, known zenith angles z (see Wilkinson 1967; Partridge *et al.* 1984). At a given zenith angle, the measured antenna temperature may be expressed as

$$T(z) = T_{CBR} + T_{gal}(z) + T_{gr}(z) + T_{atm}(z) ,$$

where T_{CBR} is the temperature of the cosmic background radiation (known to be isotropic to ~ 1 part in 10^3), T_{gal} is the (angle-dependent) radio emission of the Galaxy, and T_{gr} is the (angle-dependent) emission from the ground leaking into the side- and backlobes of the antennas we employed. At observing frequencies ≥ 10 GHz, the Galactic contribution was $\lesssim 8$ mK and hence insignificant. Observations at 9.4, 4.75, 3.7, and 2.5 GHz were corrected for Galactic emission using scaled maps made at lower frequencies (see, e.g., Sironi, Inzani, and Ferrari 1984; Mandolesi *et al.* 1986). The low side- and backlobe pickup of the corrugated horn antennas we used, plus careful screening of emission from the ground, reduced T_{gr} to negligible levels (see Partridge *et al.* 1984 for a more detailed description). For the zenith angle dependence of T_{atm} we first took $T_{atm}(z) = T_{atm}(0)$ sec z and then convolved the secant dependence with the measured beam patterns of the antennas. We also made minor corrections for the curvature of the Earth's atmosphere and for self-absorption in the atmosphere. Values of the antenna temperature contributed by the atmosphere at the zenith, $T_{atm}(0)$, were derived at each frequency from sets of corrected measurements at different values of z.

The observing site was a plateau at 3800 m elevation near the high-altitude White Mountain Research Station (Nello Pace Laboratory) of the University of California. Measurements were made in 1982 June and July, 1983 August and September, and 1984 August. Typical values of the ambient temperature were between 11 °C as a maximum and 0 °C as a minimum in summer. The barometric pressure stayed almost constant between 485 and 490 mm in this period. The long-term average relative humidity (RH) with clear sky conditions is 50% in July, 64% in August, and 60% in September. During clear days in 1983 July, RH was about 43%; it was 50% in August and 43% during the observing time in the first 10 days of September (data kindly provided by Nello Pace Laboratory staff). During the 1983 run, a solar hygrometer was available to determine the total water vapor content during daylight; with clear sky, values of precipitable water vapor (pwv) ranging from 1.6 to 4.7 mm were found. There is a decent correlation between hygrometer measures of pwv and the measured RH at the ground (Fig. 1). On the basis of these data, we can conclude that on White Mountain the water vapor content increased from the beginning of July to the end of August. It then had a maximum and began to decline in the first days of September. This behavior is very similar to that of other high-altitude observing sites in North America, such as Wheeler Peak (3.9 km altitude in Nevada), Mount Graham in Arizona, and Kitt Peak in Arizona (Wallace and Livingstone 1984).

To minimize the absorption due to liquid water droplets, we consider only measurements made both with clear sky conditions and with very high visibility; hence we expect liquid water concentrations lower than 0.001 g m^{-3} (Nilsson 1979), and we can hope to avoid problems introduced by spatial and temporal fluctuations.

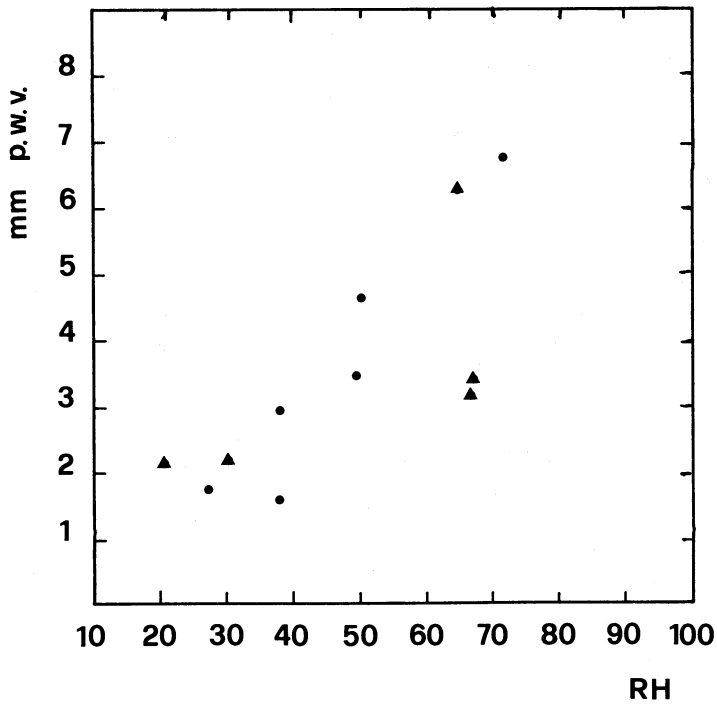

FIG. 1.—Water vapor content as measured by the solar hygrometer against the relative humidity (RH) at White Mountain. Filled triangles refer to days in 1983 August; filled circles refer to days in September.

We can divide the data at the seven frequencies into two groups. For the lowest frequencies, 2.5, 3.7, and 4.75 GHz, the water vapor contribution to T_{atm} is negligible and the oxygen contribution dominates. Likewise, at 9.4 and 10 GHz, the water vapor contribution is still much smaller than the O_2 contribution; but we can expect to see variations of 1–2 mm pwv reflected in measured values of T_{atm} at a level of about 25–50 mK. On the other hand, at 33 and 90 GHz, the water vapor contribution is extremely important and we expect to see variations in the data produced by changes as small as 0.1 mm of precipitable water vapor. The situation is presented in Table 1, where we display the results of absorption calculations based on the reference model and on a midlatitude summer model atmosphere (McClatchey *et al.* 1972). We also used other model atmospheres and find that the results reported in Table 1 are essentially insensitive to the details of the model atmospheres for frequencies up to 10 GHz; however, there is a weak dependence for the values at 33 and 90 GHz (but the variations are less than 2%).

a) Low Frequencies: $\nu \leq 10$ GHz

Table 1 shows that at lower frequencies, 2.5 and 4.75 GHz, we have practically no absorption due to water vapor or liquid water droplets at 3.8 km altitude. In fact, the histogram of all the atmosphere antenna temperatures (101 data points) at 4.75 GHz on several different days of 1983 September shows a distribution very similar to Gaussian with a mean of 997 mK and a standard deviation of 104 mK (Mandolesi *et al.* 1986). Also, the reference model predicts for the White Mountain site a contribution from the water vapor to the atmosphere antenna temperature at zenith T_{atm} of only 1 mK (mm pwv)$^{-1}$ at 2.5 GHz and 5 mK (mm pwv)$^{-1}$ at 4.75 GHz. Hence we may lump together all the low-frequency T_{atm} data regardless of the daily water vapor content. The results are $T_{atm}(2.5\ \text{GHz}) = 910$–$1000$ mK (Sironi, Inzani, and Ferrari 1984) and $T_{atm}(4.75\ \text{GHz}) = 997 \pm 60$ mK (Mandolesi *et al.* 1986). The quoted errors or uncertainties are the results of a sum in quadrature of the statistical errors (usually small) and of the estimated systematic errors. Recently De Amici *et al.* (1988) measured $T_{atm} = 870 \pm 144$ mK at 3.7 GHz in 1986, and $T_{atm} = 944 \pm 43$ in 1987, again consistent with the model. Smoot *et al.* (1987) report $T_{atm} = 850 \pm 50$ at 1.4 GHz, but this is not a direct measurement but rather an extrapolation from the 3.7 GHz measurement, which, as we have noted, is subject to a substantial correction for Galactic emission.

Assuming an average value of 3 mm pwv (on the basis of hygrometer measurements and the high-frequency data discussed below) during the observing runs, these observational results give the oxygen contributions to the atmospheric antenna temperature, $T_{ox}(2.5) = 905$–995 mK and $T_{ox}(4.75) = 983$ mK. Theoretical predictions of O_2 *line* opacity contributions are 3 mK at 2.5 GHz and 30 mK at 4.75 GHz. Thus the *nonresonant* O_2 contribution largely dominates at 2.5 and 4.75 GHz. Our data suggest that $T_{oxc}(2.5) = 902$–992 mK and $T_{oxc}(4.75) = 953 \pm 60$ mK. With these results we are in turn able to derive the width parameter τ_0. Employing equation (15), we find good agreement with the low-frequency data with $a = 0.0056$ and $b = 1.05$. These values of the parameters a and b in turn are in good agreement with the results obtained by Kaufman (1967): $a = 0.00527 \pm 0.00025$ (GHz kPa^{-1}) and $b = 0.89 \pm 0.27$. The agreement is also decent with the result found by Maryott and Birnbaum (1960), who measured a nonresonant line width of 0.0052 GHz kPa^{-1} in pure oxygen at 300 K. On the other hand, Lam (1977) and Smith (1981) proposed that the nonresonant broadening parameter has the same value as that of the resonant lines when resolved. This would require that the parameter a be $\cong 0.012$ as Liebe (1981) also claimed; in this case we would expect values of T_{atm} at 2.5 and 4.75 GHz about 2000 mK, which are clearly excluded by the White Mountain measurements. Thus these data help discriminate between the proposed theories. We note also that Rosenkranz (1982) has pointed out that the nonresonant broadening parameter is expected to be smaller than that for resonant lines, because inelastic collisions broaden bands and continua less effectively than single lines.

Further observational support for our values of the parameters a and b is provided by the measurements by De Amici *et al.* (1988) at 3.7 GHz referred to above. Our calculations are also confirmed by the data collected at 9.4 and 10 GHz. At 9.4 GHz, for instance, the weighted average of the data taken during three clear days in 1982 gave $T_{atm} = 1035 \pm 30$ mK (Partridge *et al.* 1984). On the same days an average value of 2.5 mm pwv was measured with the solar hygrometer. The reference model predicts $T_{atm} = 1134$ for these conditions. Atmospheric measurements at 10 GHz were repeated in 1983, 1984, and 1986 by the Berkeley group (see for a summary Table 3 of Kogut *et al.* 1988). The results of their observations range from $T_{atm} = 1070$ to $T_{atm} = 1300$ mK, which just spans the interval of values expected on the basis of the 9.4 GHz results and the model predictions. We can therefore conclude that the O_2 continuum attenuation is well represented by equations (14) and (15) with the values of a and b given above.

b) High Frequencies: 33 *and* 90 GHz

To discuss the atmospheric emission at 33 and 90 GHz, we will concentrate on the 1983 and 1984 data collected by the Berkeley group. However, we first mention briefly the 1982 observations. That summer, a typical value for $T_{atm}(33)$ was 5000 ± 140 mK and $T_{atm}(90) = 12{,}400 \pm 800$ mK. If we assume that the liquid water droplet contribution is still negligible at 33 and 90 GHz, we can derive, using Table 1, $T_{atm}(33) = 3545 + 340w$ and $T_{atm}(90) = 6102 + 1495w$, expressed in mK, where w is the precipitable water vapor in millimeters; hence, from the above-mentioned typical values for T_{atm}, we can estimate a typical value of 4 mm pwv, in rather good agreement with the hygrometer measurements.

Of course we expect significant variations of T_{atm} during a given day, owing to the relatively large and possibly variable contribution from water vapor to the atmospheric emission; unlike the case at lower frequencies, variations of 1 mm pwv are clearly reflected in T_{atm} (see also Table 1). It follows that accurate measurements at 33 and 90 GHz give very useful information about water vapor content. Moreover, we expect that $T_{atm}(33)$ should be well correlated with $T_{atm}(90)$. Simultaneous atmospheric scans with the 10, 33, and 90 GHz radiometers were made in several years by the Berkeley group (see Costales *et al.* 1986; Kogut *et al.* 1988); we turn to them now.

If we neglect the contribution to T_{atm} from the liquid water, we can write T_{atm} at a frequency ν simply as follows (Partridge *et al.* 1984):

$$T_{atm}(\nu) = T_{ox}(\nu) + T_{wv}(\nu)w\ . \tag{16}$$

using equation (3) with $\tau_\nu \ll 1$. Therefore the measured antenna temperatures of the atmosphere at two frequencies are con-

TABLE 1

PREDICTIONS OF OUR REFERENCE ATTENUATION MODEL CONVOLVED WITH A MIDLATITUDE SUMMER MODEL ATMOSPHERE

			O_2 LINES		O_2 CONTINUUM		H_2O LINES		H_2O CONTINUUM		H_2O	
ν (GHz) (1)	T_{atm} (mK) (2)	$\bar{T}_{phys}$ (K) (3)	τ_{ox} (nepers) (4)	T_{ox} (mK) (5)	τ_{ox} (nepers) (6)	T_{ox} (mK) (7)	τ_{wv} (nepers mm^{-1}) (8)	T_{wv} (mK mm^{-1}) (9)	τ_{wv} (nepers mm^{-1}) (10)	T_{wv} (mK mm^{-1}) (11)	$\tau_{lw} \times 10^{-3}$ (nepers mm^{-1}) (12)	$T_{lw} \times 10^{-3}$ (mK mm^{-1}) (13)
2.5	949	250	3.23E−5	8	3.75E−3	938	1.99E−6	0.5	3.61E−6	1	2.01E−6	0.5
4.75	993	250	1.12E−4	28	3.79E−3	948	7.62E−6	2	1.31E−5	3	7.25E−6	2
9.4	1158	251	4.83E−4	121	3.81E−3	956	3.97E−5	10	5.11E−5	13	2.78E−5	7
10	1180	251	5.14E−4	129	3.84E−3	956	4.74E−5	12	5.78E−5	14	3.13E−5	8
33	4661	251	1.01E−2	2534	3.99E−3	1002	5.83E−4	146	6.29E−4	158	2.80E−4	70
90	11575	253	1.89E−2	4782	5.22E−3	1320	1.22E−3	309	4.69E−3	1186	1.08E−3	274

NOTE.—Vertical path from a 3.8 km altitude observing site; the model atmosphere predicts 3.7 mm pwv. T_{atm} is the zenith atmosphere antenna temperature computed neglecting any contribution from liquid water droplets. $\bar{T}_{phys}$ is defined by eq. (3). The table shows the attenuations and the contributions to T_{atm} due to oxygen and water vapor lines and continua; in cols. (12) and (13) we present separately the liquid water droplet contributions.

nected in the case of simultaneous measurements by the relation

$$T_{atm}(\nu_1) = \left[T_{ox}(\nu_1) - \frac{T_{wv}(\nu_1)T_{ox}(\nu_2)}{T_{wv}(\nu_2)} \right] + \frac{T_{wv}(\nu_1)}{T_{wv}(\nu_2)} T_{atm}(\nu_2) = \beta + \alpha T_{atm}(\nu_2) , \quad (17)$$

with slope α and intercept β so defined (Costales *et al.* 1986). We emphasize that these simultaneous measurements allow a direct comparison of the atmospheric absorption at two different frequencies, bypassing the need to determine the precipitable water vapor content. We thus avoid uncertainties introduced by spatial and temporal variations in H_2O and its poor correlation with relative humidity. For this reason, we rely strongly on the simultaneous measurements (and we will see in § IV that they require adjustments to the reference model).

Costales *et al.* (1986) computed the correlations between 10 and 33 GHz, 10 and 90 GHz, and 33 and 90 GHz data collected both in Berkeley (altitude 250 m) and at White Mountain. We must, however, use these results with some caution. In the $T_{atm}(33)$ versus $T_{atm}(90)$ relationship, it is preferable to use only data collected with clear sky and hence low water vapor content, because small temporal or spatial variations of precipitable water vapor could result in significant variations of $T_{atm}(90)$ and $T_{atm}(33)$. On the contrary, when $T_{atm}(10)$ is involved in the correlations, we also need data obtained in the presence of high pwv content to get a significant correlation (see, e.g., Fig. 7 of Costales *et al.* 1986). If, as is likely, the distribution of the water vapor is irregular when pwv is high, the systematic errors connected with the use of the secant law will increase rapidly with increasing water vapor content. Nevertheless, all the data do show strong correlations, as expected. This fact suggests that even without clear sky conditions the correlation holds. In this paper, however, we have chosen to confine ourselves to examining 33 and 90 GHz data only when the measured or predicted (on the basis of the reference model) water vapor content is less than 6 mm. Then, as Figure 1 shows, this limit should ensure a low value of relative humidity at the ground and a high visibility. We hope in this way to avoid temporal and spatial fluctuations and a significant influence of liquid water droplets on the emission from the atmosphere at high frequency. Recently, Kogut *et al.* (1988) reexamined all the 10 and 90 GHz simultaneous measurements and found that $\alpha_{10,90} = 0.013 \pm 0.005$ and $\beta = 1012 \pm 75$, in good agreement with the reference model which predicts $\alpha_{10,90} = 0.017$ and $\beta = 979$. On the other hand, the simultaneous observations at 33 and 90 GHz give $\alpha_{33,90} = 0.232 \pm 0.014$ and $\beta = 1917 \pm 150$; the reference model predicts 0.203 and 2297.

In the latter case, the discrepancy between the data and the predictions is clear, although not dramatic. It is also interesting to note that, using the reference model and the 1983 quasi-simultaneous observations at 33 and 90 GHz to compute the water vapor content, we find some discrepancies; the water vapor content computed with the 90 GHz data is usually higher than that computed with 33 GHz data, and both are higher than the hygrometer measurements.

It is clear from § II that the number of parameters involved in the reference model calculation is high ($\simeq 500$); nevertheless, we can try to understand the partial failure of the reference model and eliminate some possibilities. A first possibility is the presence of an appreciable quantity of liquid water in droplets. Let us assume, for instance, that we have a concentration 10^{-3} g m^{-3} of liquid water vapor in droplets (this is usually assumed as the limiting value between clear sky and haze) in the first 2000 m above our equipment on White Mountain. Then we have to add to T_{atm} the corresponding contribution from aerosols; from Table 1 we find this is $\simeq 140$ mK at 33 GHz and $\simeq 550$ mK at 90 GHz. It is easy to see that these contributions neither change the slope predicted by the model nor change the intercept in the right way.

IV. ADJUSTING THE REFERENCE MODEL

At this point we have to examine the hypothesis that the reference model used to compute the H_2O and/or O_2 contributions to T_{atm} is not adequate for some reason.

a) *Correcting the Water Vapor Contribution*

Beginning with the H_2O contribution, we notice that the reference model predicts slopes smaller than observed ones. Taking into account the relative importance of the various contributions to τ_{wv} (see Table 1), one could imagine reducing the continuum contribution by the same factor for all the frequencies; in fact, a reduction factor of 0.6 will result in a slope for the $T_{atm}(33)$–$T_{atm}(90)$ relationship in agreement with the observations. On the other hand, this solution would further increase the predicted values of the water vapor content, and with the reference model we already get values of pwv higher than those measured with the hygrometer. Moreover, this solution would increase the discrepancy in the water vapor predictions based on the 33 and 90 GHz measurements. Of course, an *increase* by a frequency-independent factor of the H_2O continuum contribution to T_{atm} would decrease the slope of the $T_{atm}(33)$–$T_{atm}(90)$ relationship, making the agreement with the observations even worse.

We next consider the possibility that the disagreement comes from an error in the H_2O *line* contribution due to uncertainties in the line parameters or line shapes. If in our reference model we have underestimated the theoretical line strength for the 22.235 GHz H_2O line by 20% (cf. Liebe 1985), we must correct the estimates of the water vapor contribution at 10 GHz to $T_{wv}(10) = 28$ mK (mm pwv)$^{-1}$, and at 33 GHz to $T_{wv}(33) = 333$ mK (mm pwv)$^{-1}$. There is no appreciable change in $T_{wv}(90)$, hence the predicted slope $\alpha_{33,90} = 0.223$ is now in good agreement with the slope of the data. The data we have available thus suggest that the 22.235 GHz line strength is 20% larger than predicted by the reference model. A correction of only 10% would give $\alpha_{33,90} = 0.213$ and $\beta = 2110$, deviating from the observations significantly; also, a correction factor as large as 30% would cause a disagreement with the H_2O opacities found at 20.6 and 31.6 GHz by Hogg, Guiraud, and Westwater (1983) and Liebe (1985).

In the discussion above, we considered simply scaling the H_2O continuum contribution to the atmospheric emission by a constant factor. In fact, the difference between the Gaut and Rafenstein (1971) expression for the continuum and Liebe's expression is basically a constant. However, there are other proposed expressions for the continuum contribution which have different dependences on the frequency, on the temperature, and on the water vapor content. Indeed, the most significant dependence is on the frequency. Usually these expressions have been derived at frequencies higher than 200 GHz (where O_2 opacity begins to become negligible) and are strictly dependent on the choice of the line shape (see § V

below). However, we can extrapolate them to lower frequencies, to check whether different frequency dependences of the continuum can help in reconciling the models and the data.

Zammit and Ade (1981) proposed a flatter $\nu^{1.22}$ dependence, compared with the classical ν^2 dependence. If we use their expression to compute the H_2O continuum contribution to T_{atm}, we find a contribution of about 150 mK (mm pwv)$^{-1}$ at 10 GHz, 635 mK (mm pwv)$^{-1}$ at 33 GHz, and 2160 mK (mm pwv)$^{-1}$ at 90 GHz. These values can be rejected on the basis of the data (slope of $T_{atm}(33)$–$T_{atm}(90)$ correlation and computed water vapor content).

Burch (1982) proposed a steeper $\nu^{2.5}$ dependence on frequency; his model gives a continuum contribution of about 3 mK (mm pwv)$^{-1}$ to $T_{atm}(10)$, of about 60 mK mm^{-1} to $T_{atm}(33)$ and of about 720 mK mm^{-1} to $T_{atm}(90)$. The result is an even lower slope than for the reference model, making the agreement with the observations worse.

We conclude that none of the suggested changes to the *continuum* contribution helps bring the reference model into better agreement with the observations. On the other hand, a 20% increase in the *line* strength of the prominent 22 GHz line does improve the fit to the data. We adopt this as part of our *adjusted model* for atmospheric emission.

b) *Correcting the O_2 Contribution*

The changes in the slopes of predicted linear correlations do not solve the problem of the *intercepts*. In particular, the value derived for the $T_{atm}(33)$–$T_{atm}(90)$ correlation suggests higher values of the oxygen contribution at 90 GHz. This contradicts Stankevich's (1974) suggestion that at frequencies higher than 60 GHz the O_2 continuum attenuation vanishes. If this were true, the intercept would be farther off and the predicted water vapor contents more discrepant.

On the other hand, an increase by a constant factor of the O_2 continuum attention will not solve the problem either, because the O_2 continuum contribution to T_{atm} is much more important at 33 GHz than at 90 GHz. Again we are left with the possibility that the *line* contributions in the wings are not well described by the reference model.

In particular, for 3.8 km altitude observations, the main contribution to the O_2 opacity comes from the band at 60 GHz, rather than from the 118 GHz line, for our working frequencies. With a physical temperature of the atmosphere $T_{phys} = 261$ and a total pressure $P = 487$ mbars (conditions similar to our observing conditions), the contribution of the 60 GHz band to the 90 GHz attenuation is about 10 times the contribution of the 118 GHz line.

The contribution of the 60 GHz band to the O_2 attenuation is the sum of the positive and negative contributions of the 41 component lines; many of these contributions have absolute values equal to or higher than the total attenuation in the whole band. Therefore, errors of a few percent in the evaluation of the line parameters (particularly for the interference coefficients) can result in significant errors in the evaluation of the opacity in the wings of the band. Thus it is not implausible that the reference model could underestimate the O_2 line contribution at 90 GHz by, say, 15%. If we increase the O_2 line contribution predicted by the reference model at 90 GHz by 1.15, we get $T_{atm}(90) = 6800$ mK, in better agreement with the White Mountain observations. An increase of 25% would actually bring the observed and computed intercepts into better agreement, but a value this high would contradict the experimental data on the 60 GHz band (Reber 1972 and Liebe 1975). We adopt a 15% increase in the 60 GHz O_2 line strength as part of our *adjusted model*.

c) *Adjusted Model*

These two adjustments of the reference model lead to the following relationships for our observations at 3800 m, expressed in mK:

$$\begin{aligned} T_{atm}(2.5) &= 946 + 2w\,, \\ T_{atm}(4.75) &= 976 + 5w\,, \\ T_{atm}(9.4) &= 1077 + 26w\,, \\ T_{atm}(10) &= 1085 + 28w \\ T_{atm}(33) &= 3545 + 333w\,, \\ T_{atm}(90) &= 6800 + 1495w\,. \end{aligned} \tag{18}$$

The main changes to the reference model are in the oxygen contribution to T_{atm} at 90 GHz, which changes from 6102 to 6800 mK, and in the contribution per millimeter of pwv at 33 GHz, which increases from 304 to 333 mK. With respect to Liebe's "millimeter propagation model" (1985), there is the further difference that we do not damp the oxygen continuum at high frequencies (see § II*b*). These differences result in an 11% increase of the water vapor contribution at 33 GHz for a 3.8 km altitude site, and a 26% increase for the dry air contribution at 90 GHz. The adjusted model gives $\alpha_{33,90} = 0.223$, $\beta_{33,90} = 2030$ and $\alpha_{10,90} = 0.018$, $\beta_{10,90} = 967$, within the 1 σ error bars of the observational results. These values provide acceptable fits to the observed data. Moreover, if we use this adjusted model and the values of T_{atm} obtained at 33 and 90 GHz in 1983, we derive values of water vapor content which are in agreement with the hygrometer measurements.

The above relationships (eq. [18]) differ very little from the previous ones presented by Partridge *et al.* (1984) at low frequencies, but the differences become appreciable at 33 and 90 GHz, both in the oxygen and in the water vapor terms. The main reason for differences in the water vapor terms is the use here of a new expression for the water vapor continuum (eq. [9]), which has a normalization smaller by about 30% than Gaut and Rafenstein's classical formula, and also has a slightly different dependence on the temperature (2.5 instead of 3.1). Also, the oxygen contribution has been computed here with a different recipe, using a richer data base particularly for the interference coefficients of the lines (cf. § II). Our relationships (eq. [18]) at 33 and 90 GHz also differ substantially from those adopted by Costales *et al.* (1986) for essentially the same reasons. These authors also noted disagreements between the observed values and the model predictions. They made the ad hoc suggestion that changing the H_2O contribution at 90 GHz to 1540 mK mm^{-1} would help bring the predictions into better accord with the observations—this value is very close to the one we get.

Finally, we must add that the model we chose as a reference has already passed a number of observational tests (see, e.g., Waters 1976; Smith 1981; Liebe 1985); our proposed adjustments do not spoil this property of the model. Comparing our model with the body of available data on zenith opacity, we find that almost all the experimental results are reproduced by our model to 5% accuracy at low frequencies and 10% accuracy at high frequencies. In the next section we will list some atmospheric measurements of astronomical interest together with the model predictions, to substantiate this claim (see Tables 2–4).

TABLE 2

LOW-FREQUENCY MEASUREMENTS COMPARED WITH PREDICTIONS FROM REFERENCE MODEL

Source	ν (GHz)	τ_{obs} (dB)	τ_{mod} (dB)	T_{obs} (K)	T_{mod} (K)
Howell and Shakeshaft 1967	0.408	0.016 ± 0.007	0.020	...	...
Howell and Shakeshaft 1967	1.4	0.034 ± 0.008	0.035	...	...
Encrenaz, Penzias, and Wilson 1970	1.4	0.035 ± 0.002	0.035	...	...
Ohm 1961	2.39	...	...	2.3 ± 0.2	2.21
Medd and Fort 1966	3.20	0.042 ± 0.004	0.038	...	...
Penzias and Wilson 1965	4.08	...	...	2.3 ± 0.2	2.35
De Grasse *et al.* 1959	5.65	...	...	2.5 ± 0.75	2.49
Hogg and Semplak 1961	6.0	...	...	2.8	2.53
Roll and Wilkinson 1966	9.34	...	...	3.0 ± 0.2	3.04

d) Comparison of Adjusted Model with Other Previous Data

With the aim of further testing the adjusted model, we can compare its predictions with the observational results for zenith opacity (or zenith atmosphere temperature) at low frequencies, where the variable water vapor contents are relatively unimportant even for measurements performed at sea level. At these frequencies we are therefore able to test the attenuation due to the oxygen continuum.

The data and predictions presented in Table 2 are in very good agreement, and this again confirms the reliability of the adjusted model at low frequencies.

Further interesting comparisons are possible because White Mountain has been used several times as the observing site for experiments on the CBR spectrum. The previous atmospheric emission measurements made in connection with these observations from White Mountain are listed in Table 3 along with the adjusted model results; we also present the typical range of pwv in millimeters, computed from the range in T_{obs} on the basis of the adjusted model.

The water vapor contents in column (5) are reasonable, except those calculated from the 9.37 GHz measurements. Values of water vapor content higher than 10 mm pwv on White Mountain are in our experience connected with cloudy sky conditions only. Another possibility is angle-dependent pickup from the ground (see § III). Since the antennas used by Stokes, Partridge, and Wilkinson (1967) had larger side- and backlobes than the corrugated horns we used, it is possible that zenith-angle–dependent pickup from the ground somehow mimicked the secant z dependence of atmospheric emission, leading to an overestimate of the latter.

There is one more atmospheric emission determination connected with CBR spectrum measurements which strongly contrasts with the model predictions. Boynton and Stokes (1974) performed an airborne CBR spectrum experiment at 90 GHz; they found at an altitude of 14–15 km $T_{atm}(90) = 1.21 \pm 0.37$, whereas the adjusted model predicts $T_{atm}(90) = 0.245$. The reason for this large discrepancy is not clear to us.

V. MODEL PREDICTIONS OF ZENITH ATTENUATION AT MAUNA KEA, KITT PEAK, AND THE SOUTH POLE

The adjusted model can also be used to predict opacities at frequencies higher than 200 GHz, where water vapor optical depth dominates. It is particularly interesting to compare the model predictions with the data taken at 212–408 GHz by Zammit and Ade (1981) and with the empirical correction for the water vapor excess proposed by Rice and Ade (1979) (see Table 4).

Zammit and Ade (1981) collected their data at a mountain site (2.4 km altitude), Izana in Tenerife, Canary Islands, during 1980 August, with water vapor contents ranging from 4.3 to 14 mm pwv. It is easy to see that the oxygen attenuation for their experimental situation is only a few percent of the total attenuation; thus differences in computing the oxygen attenuation are irrelevant. It is therefore interesting to notice that the fit to the data obtained with our adjusted model is as good as that obtained by Zammit and Ade. Recall that the attenuation per millimeter of water vapor is the sum of line and continuum contributions. Zammit and Ade used the Gross (1955) line shape and Rice and Ade's (1979) expression for the continuum, whereas we used the line shape reproduced above as equation (5) and values of a and b deduced from our low-frequency data. It must be stressed that the empirically defined expression for the continuum depends on the assumed line shapes.

In the range of frequencies tested by Zammit and Ade both the models are reliable (see Table 4), but Liebe's recipe for the continuum has the advantage that it also gives a good fit to the data at lower frequencies (see discussion in § IV above).

In the millimeter range, many measurements have been made from various sites, particularly from Mauna Kea and Kitt Peak, where millimeter telescopes are operating.

TABLE 3

MEASUREMENTS AND PREDICTIONS FROM WHITE MOUNTAIN SITE
(3.8 km altitude)

Source (1)	ν (GHz) (2)	T_{obs} (K) (3)	T_{mod} (K) (4)	Calculated pwv (mm) (5)
Stokes, Partridge, and Wilkinson 1967	9.37	1.37 ± 0.1	$1.07 + 0.025w$	7.2–15
Stokes, Partridge, and Wilkinson 1967	19	2.85–4.12	$1.53 + 0.456w$	2.9–5.7
Welch *et al.* 1967	20	4.0 ± 0.2	$1.63 + 0.810w$	2.7–3.2
Ewing, Burke, and Staelin 1967	32.5	3.84–5.59	$3.46 + 0.339w$	1.1–6.3
Wilkinson 1967	35	5.71–7.48	$4.24 + 0.335w$	4.4–9.6

TABLE 4

ATTENUATION (dB mm^{-1}) FROM WATER VAPOR

ν (GHz)	Observed Attenuation, H_2O Only[a]	H_2O Lines Only (gross shape)	H_2O Lines Only[b]	H_2 Lines + Continuum[c]	Our Model[d]
212.40.....	0.239 ± 0.006	0.125	0.077	0.240	0.217
229.63.....	0.244 ± 0.005	0.127	0.066	0.254	0.231
252.60.....	0.281 ± 0.004	0.154	0.077	0.297	0.276
287.04.....	0.380 ± 0.006	0.228	0.126	0.394	0.382
344.65.....	0.813 ± 0.012	0.607	0.436	0.812	0.836
407.60.....	1.507 ± 0.057	1.202	1.000	1.455	1.518

[a] From Zamit and Ade 1981; corrected to H_2O only.
[b] Line shapes from eq. (5).
[c] Line shapes from Gross 1955; continuum from Rice and Ade 1979.
[d] Line shapes from eq. (5); continuum from Liebe 1984.

De Zafra *et al.* (1983) measured the zenith attenuation at 1.1 mm wavelength on different days in 1982 at Mauna Kea (4.2 km altitude) and derived the water vapor content, using Rice and Ade's result for 287 GHz [0.0876 nepers mm pwv)$^{-1}$]. This is a little misleading in the sense that Rice and Ade neglected the oxygen contribution (no longer negligible with very low water vapor content) and that they used a H_2O contribution to the attenuation observed from a 2.4 km altitude site. Our adjusted model, which as we see from Table 4 fits Zammit and Ade's value at 287 GHz, gives an attenuation $1.26 \times 10^{-2} + 6.0 \times 10^{-2} w$ (nepers) at the altitude of Mauna Kea; thus, for example, a measured attenuation of 0.1 nepers corresponds to 1.46 mm pwv, instead of 1.14 as claimed by De Zafra *et al.* (1983).

Cota and Sramek (1984) measured the atmospheric attenuation at 225 GHz at Kitt Peak in 1984 June and July. With clear sky conditions, they found values of attenuation ranging from 0.211 to 0.799 nepers, with an average value of 0.449 nepers. The reference model predicts for Kitt Peak a total opacity $\tau = 1.62 \times 10^{-2} + 5.42 \times 10^{-2} w$ (nepers). Thus the observed values correspond to a water vapor content ranging from 3.6 to 14 mm pwv, with an average of 8 mm, in agreement with the water vapor contents derived from Tucson Rawisond data and from the equivalent widths of the H_2O 1.0832 μm line as found by Wallace and Livingstone (1984).

The adjusted model also predicts for the Kitt Peak site a total opacity $\tau = 2.09 \times 10^{-2} + 7.96 \times 10^{-2} w$ (nepers) at 300 GHz. In Figures 2 and 3 we present the computed zenith opacity due to water vapor and oxygen in the frequency range 10–380 GHz (3 cm–0.8 mm wavelength) for Mauna Kea, Kitt Peak, and the Amundsen-Scott South Pole Station (2835 m elevation).

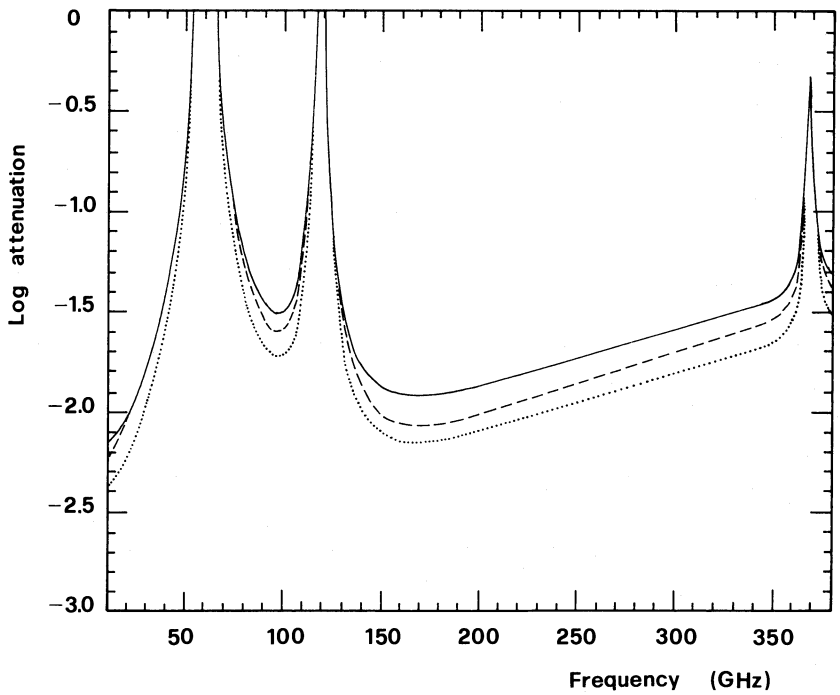

FIG. 2.—Adjusted model predictions of the zenith attenuation in nepers due to oxygen at a site with 2040 m altitude like Kitt Peak (*solid line*), a site with 2800 m altitude like the Amundsen-Scott Station at the South Pole (*dashed line*), and a site with 4200 m elevation like Mauna Kea (*dotted line*). The average physical temperature (see eq. [3]) in the 30 GHz window is 254 K for Kitt Peak and Mauna Kea and 235 K for the Amundsen-Scott Station; in the 90 GHz window, it is 260 K for Kitt Peak and Mauna Kea and 238 K for the Amundsen-Scott Station; in the window region between 200 and 380 GHz, it is 260 K for Kitt Peak and Mauna Kea and 244 K for the Amundsen-Scott Station.

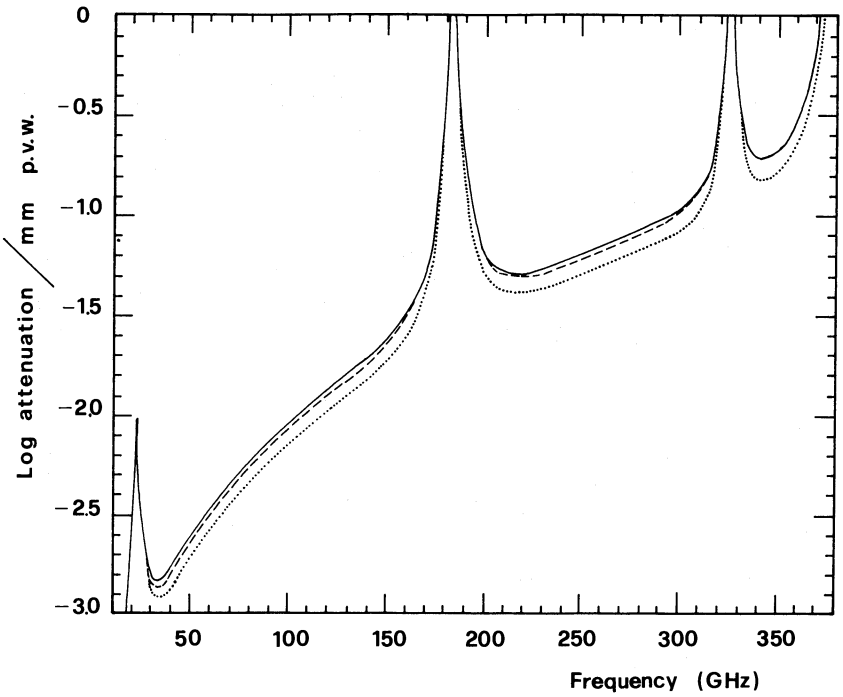

FIG. 3.—Adjusted model predictions of zenith attenuation in nepers per millimeter of precipitable water vapor for Kitt Peak (*solid line*), for the South Pole (*dashed line*), and for Mauna Kea (*dotted line*).

In Figure 2 the oxygen optical depth τ_{ox} is reported in nepers, while in Figure 3 the water vapor attenuation τ_{wv} in nepers per millimeter of pwv is shown. The zenith optical depth can be calculated by the following relationship

$$\tau = \tau_{ox} + \tau_{wv} w .$$

To compute the atmospheric antenna temperature one can use equation (3), with the values of T_{phys} reported in the figure captions.

As is apparent from the figures, the oxygen opacity at Kitt Peak (2040 m elevation) is $\sim$60% larger than at Mauna Kea (4200 m elevation), whereas the water vapor attenuation per millimeter of pwv changes by only 25%. On the other hand, at the Amundsen-Scott Station the water vapor attenuation per millimeter of pwv is $\sim$20% higher than at Mauna Kea, but the typical value of precipitable water vapor is lower, about 0.5 mm, compared with 2 mm. Moreover, the average physical temperature of the atmosphere is lower at the South Pole. Therefore, the average zenith temperature due to the water vapor is a factor of 3–4 lower at the Amundsen-Scott Station than at Mauna Kea. This fact is particularly relevant for the windows between 200 and 400 GHz, where the water vapor contributes almost the entire opacity. However, a low contribution of water vapor opacity is also very important for measurements of the spectrum and the small-scale anisotropy of the cosmic background radiation in the windows around 30 and 90 GHz. The spatial and temporal variability of the water vapor optical depth is one of the major problems in this kind of measurement. Hence it is important to minimize the absolute contribution of the water vapor, and thus the amplitude of its variations. On the other hand, it is worth noting that the minimum in the contribution from unresolved radio sources to the microwave background anisotropy at small (from 1′ to 1°) angular scales falls in the frequency range $\sim$30 to $\sim$120 GHz. Therefore, the Amundsen-Scott Station is potentially a very interesting site for ground-based measurements of small-scale fluctuations of the CBR.

VI. CONCLUSIONS

High-precision data taken at White Mountain over many years provide interesting constraints on theoretical models of atmospheric attenuation. The low-frequency data ($\leq$10 GHz) allow us to make an accurate determination of the O_2 continuum contribution. Using these results, we are able to test a model which at low frequencies has typical uncertainties of only $\sim$5%.

The simultaneous measurements of atmospheric emission made at 10, 33, and 90 GHz suggest that the reference model probably underestimated by 20% the contribution to the total opacity of the 22 GHz line of H_2O and by 15% the contribution of the 60 GHz band of O_2. We propose an adjusted model (§ IV), which fits the simultaneous observations at 10, 33, and 90 GHz; it also has the advantage of bringing the water vapor contents determined from both the 33 and the 90 GHz data into agreement with hygrometer measurements.

Our data also help to confirm over a large range of frequencies (a few GHz to a few hundred GHz) and altitudes the expression for the H_2O continuum proposed by Liebe (1985). Other empirical solutions of the EWA problem are not able to give good fits to the low-frequency data.

Our adjusted model results also agree with the observations made at millimeter wavelengths from Mauna Kea and Kitt Peak. The attenuations in the 1–380 GHz frequency range have been computed for both sites, and for the South Pole, and are presented in Figures 2 and 3.

We are very grateful to H. J. Liebe for his illuminating remarks and suggestions, and to G. De Amici for a very careful

reading of this paper. We are also deeply indebted to the Nello Pace Laboratory staff, who gave us great support during our observing campaigns. We also acknowledge all participants in the White Mountain collaboration; special thanks are due to J. Costales and G. De Amici for sending us the 1984 results in tabular form.

REFERENCES

Boynton, P. E., and Stokes, R. A. 1974, *Nature*, **247**, 528.
Burch, D. E. 1982, Ford Aerospace and Communications Corp., Aeronutronic Div., Final Rept. AFGL-TR-81-0300.
Chang, A. T., and Wilheit, T. T. 1979, *Radio Sci.*, **14**, 793.
Costales, J. 1984, A.B. thesis, Lawrence Berkeley Laboratory, University of California.
Costales, J., Smoot, G. F., Witebsky, C., De Amici, G., and Friedman, S. D. 1986, *Radio Sci.*, **21**, 47.
Cota, S. A., and Sramek, R. 1984, Millimeter Array Memo No. 19, NRAO internal report.
De Amici, G., Smoot, G. F., Aymon, J., Bersanelli, M., Kogut, A., Levin, S. M., and Witebsky, C. 1988, *Ap. J.*, **329**, 556.
De Amici, G., Smoot, G. F., Friedman, S. D., and Witebsky, C. 1985, *Ap. J.*, **298**, 710.
De Amici, G., Witebsky, C., Smoot, G. F., and Friedman, S. 1984, *Phys. Rev. D*, **29**, 2673.
Deepak, A., Wilkerson, T. T., and Ruhnke, L. H., eds. 1980, *Atmospheric Water Vapor* (New York: Academic).
De Grasse, R. W., Hogg, D. C., Ohm, E. A., and Scovil, H. E. D. 1959, *J. Appl. Phys.*, **30**, 2013.
de Zafra, R. L., Parrish, A., Solomon, P. M., and Barret, J. W. 1983, *Internat. J. Infrared Millimeter Waves*, **4**, 757.
Encrenaz, P. J., Penzias, A. A., and Wilson, R. W. 1970, *Astr. Ap.*, **9**, 51.
Ewing, M. S., Burke, B. F., and Staelin, D. H. 1967, *Phys. Rev. Letters*, **19**, 1251.
Flaud, J. M., Camy-Peyret, C., and Toth, R. A. 1981, in *Water Vapor Line Parameters from Microwave to Medium Infrared* (Oxford: Pergamon).
Friedman, S. D. 1984, Ph.D. thesis, Lawrence Berkeley Laboratory, University of California.
Friedman, S. D., Smoot, G. F., De Amici, G., and Witebsky, C. 1984, *Phys. Rev. D*, **29**, 2677.
Gaut, N. E., and Rafenstein, E. C., III. 1971, *Environmental Res. Tech. Rept.*, No. 13 (Lexington, MA).
Gross, E. P. 1955, *Phys. Rev.*, **97**, 395.
Hogg, D. C., Guiraud, F. O., and Westwater, E. R. 1983, *Radio Sci.*, **18**, 1295.
Hogg, D. C., and Semplak, P. A. 1961, *Bell System Tech. J.*, **40**, 1331.
Howell, T. F., and Shakeshaft, J. R. 1967, *J. Atm. Terr. Phys.*, **29**, 1559.
Johnson, D. G., and Wilkinson, D. T. 1987, *Ap. J. (Letters)*, **313**, L1.
Kaufman, I. A. 1967, Ph.D. thesis, Columbia University.
Kogut, A., *et al.* 1988, *Ap. J.*, **325**, 1.
Lam, K. S. 1977, *J. Quant. Spectrosc. Rad. Transf.*, **17**, 335.
Liebe, H. J. 1975, *IEEE Trans.*, **MTT-23**, 380.
———. 1981, *Radio Sci.*, **16**, 1183.
———. 1984, *Internat. J. Infrared Millimeter Waves*, **5**, 207.
———. 1985, *Radio Sci.*, **20**, 1069.
Liebe, H. J., Gimmestad, G. G., and Hopponen, J. D. 1977, *IEEE Trans.*, **AP-25**, 327.
Mandolesi, N., Calzolari, P., Cortiglioni, S., and Morigi, G. 1984, *Phys. Rev. D*, **29**, 2680.
Mandolesi, N., Calzolari, P., Cortiglioni, S., Morigi, G., Danese, L., and De Zotti, G. 1986, *Ap. J.*, **310**, 561.
Maryott, A. A., and Birnbaum, G. 1960, *J. Chem. Phys.*, **32**, 686.
McClatchey, R. A., Fenn, R. W., Selby, J. E. A., Volz, F. E., and Garing, J. S. 1972, *AFCRL Environmental Res. Rept.*, No. 411.
Medd, W. J., and Fort, D. N. 1966, *J. Geophys. Res.*, **71**, 4749.
Mizushima, M. 1982, *Internat. J. Infrared Millimeter Waves*, **3**, 379.
Nilsson, B. 1979, *Appl. Optics*, **18**, 3457.
Ohm, E. A. 1961, *Bell System Tech. J.*, **40**, 419.
Partridge, R. B., *et al.* 1984, *Phys. Rev. D*, **29**, 2683.
Penzias, A. A., and Wilson, R. W. 1965, *Ap. J.*, **142**, 419.
Peterson, J. B., Richards, P. L., and Timusk, J. 1985, *Phys. Rev. Letters*, **55**, 332.
Poynter, R. L., and Pickett, H. M. 1981, JPL Pub. 80-23, Rev. 1 (Pasadena: JPL).
Reber, E. E. 1972, *Geophys. Res.*, **77**, 3831.
Rice, D. P., and Ade, P. A. R. 1979, *Infrared Phys.*, **29**, 575.
Roll, P. G., and Wilkinson, D. T. 1966, *Phys. Rev. Letters*, **16**, 405.
Rosenkranz, P. W. 1975, *IEEE Trans.*, **AP-23**, 498.
———. 1982, *J. Chem. Phys.*, **77**, 2216.
Rothman, L. S., *et al.* 1983, *Appl. Optics*, **22**, 2247.
Sironi, G., Inzani, P., and Ferrari, A. 1984, *Phys. Rev. D*, **29**, 2686.
Smith, E. W. 1981, *J. Chem. Phys.*, **74**, 6658.
Smoot, G. F., *et al.* 1983, *Phys. Rev. Letters*, **51**, 1099.
Smoot, G. F., *et al.* 1985, *Ap. J. (Letters)*, **291**, L23.
Smoot, G. F., Bensadoun, M., Bersanelli, M., De Amici, G., Kogut, A., Levin, S., and Witebsky, C. 1987, *Ap. J. (Letters)*, **317**, L45.
Stankevich, K. S. 1974, *Radiophys. Quantum Electronics*, **17**, 579.
Stokes, R. A., Partridge, R. B., and Wilkinson, D. T. 1967, *Phys. Rev. Letters*, **19**, 1199.
Van Vleck, J. H. 1947, *Phys. Rev.*, **71**, 413.
Van Vleck, J. H., and Weisskopf, V. F. 1945, *Rev. Mod. Phys.*, **17**, 227.
Wallace, L., and Livingstone, W. 1984, *Pub. A.S.P.*, **96**, 182.
Waters, J. W. 1976, in *Methods of Experimental Physics*, Vol. **12B**, ed. M. L. Meeks (New York: Academic), p. 142.
Weiss, R. 1980, *Ann. Rev. Astr. Ap.*, **18**, 489.
Welch, W. J., Keachie, S., Thornton, D. D., and Wrixon, G. 1967, *Phys. Rev. Letters*, **18**, 1068.
Wilkinson, D. T. 1967, *Phys. Rev. Letters*, **19**, 1195.
Witebsky, C., Smoot, G., De Amici, G., and Friedman, S. 1986, *Ap. J.*, **310**, 145.
Zammit, C. C., and Ade, P. A. 1981, *Nature*, **293**, 550.
Zrazhevskiy, A. Y. 1976, *Radio Eng. Electronic Phys.*, **21**, 31.

L. DANESE: Istituto di Astronomia, Vicolo dell'Osservatorio 5, 35122 Padova, Italy

R. B. PARTRIDGE: Haverford College, Haverford, PA 19041